Towards a self-consistent dynamical nuclear model

2017 J. Phys. G: Nucl. Part. Phys. 44 044001

(http://iopscience.iop.org/0954-3899/44/4/044001)

IOP Publishing Journal of Physics G: Nuclear and Particle Physics
J. Phys. G: Nucl. Part. Phys. **44** (2017) 044001 (21pp) https://doi.org/10.1088/1361-6471/aa5669

Towards a self-consistent dynamical nuclear model

X Roca-Maza[1,2,4], Y F Niu[2,3], G Colò[1,2] and P F Bortignon[1,2]

[1] Dipartimento di Fisica, Università degli Studi di Milano, Via Celoria 16, I-20133 Milano, Italy
[2] INFN, Sezione di Milano, Via Celoria 16, I-20133 Milano, Italy
[3] ELI-NP, Horia Hulubei National Institute for Physics and Nuclear Engineering, 30 Reactorului Street, RO-077125, Bucharest-Magurele, Romania

E-mail: xavier.roca.maza@mi.infn.it

Received 21 October 2016, revised 15 December 2016
Accepted for publication 3 January 2017
Published 21 February 2017

Abstract

Density functional theory (DFT) is a powerful and accurate tool, exploited in nuclear physics to investigate the ground-state and some of the collective properties of nuclei along the whole nuclear chart. Models based on DFT are not, however, suitable for the description of single-particle dynamics in nuclei. Following the field theoretical approach by A Bohr and B R Mottelson to describe nuclear interactions between single-particle and vibrational degrees of freedom, we have taken important steps towards the building of a microscopic dynamic nuclear model. In connection with this, one important issue that needs to be better understood is the renormalization of the effective interaction in the particle-vibration approach. One possible way to renormalize the interaction is by the so-called *subtraction method*. In this contribution, we will implement the subtraction method in our model for the first time and study its consequences.

Keywords: nuclear density functional theory and extensions, particle vibration coupling model, subtraction method, giant resonances and sum rules

(Some figures may appear in colour only in the online journal)

[4] This article belongs to the special issue: emerging leaders, which features invited work from the best early-career researchers working within the scope of *J. Phys.* G. This project is part of the *Journal of Physics* series' 50th anniversary celebrations in 2017. Xavier Roca-Maza was selected by the Editorial Board of *J. Phys.* G as an Emerging Leader.

0954-3899/17/044001+21$33.00

1. Introduction

In our research group, we are interested in developing a microscopic nuclear structure model that can eventually also be applied to nuclear reactions. Such an achievement would solve a long-standing problem in theoretical nuclear physics [1].

We have recently developed two different energy density functionals (EDFs) [2, 3] based on density functional theory [4–6]. In nuclear physics, EDFs are commonly derived in an approximate way from a phenomenological interaction solved via the Hartree (H) or Hartree–Fock (HF) approximations [7, 8]. Such types of models are very helpful in understanding different nuclear properties, such as nuclear masses and sizes, as well as the excitation energy of nuclear collective states such as giant resonances. In the latter case, a minimal extension of the theory is needed. That is, one needs to perturb the ground state density according to the oscillation mode under study. For that purpose, one may apply the small amplitude limit of the time-dependent H or HF approximations (TDHF), which coincides with the linear response theory (LRT) or the random phase approximation (RPA) [9–11]. We have devoted our efforts to the detailed study of such observables providing, in some cases, useful theoretical guidance [12–20].

Approaches to the description of the nucleus based on nucleon–nucleon interaction in the vacuum are successful in their predictions of some properties in light and medium mass nuclei, but face computational limitations in the description of heavy systems and high-lying excited states [21–27]. However, EDF approaches do not suffer from such limitations. Nevertheless, nuclear EDFs based on static effective potentials are not suitable for the description of single-particle dynamics in the nuclei. For example, the fragmentation of single-particle states [28, 29] and their finite half-life are unequivocal finger prints. Following the field theoretical approach by A Bohr and B R Mottelson[5] [30, 31] for describing nuclear interactions between single-particle and vibrational degrees of freedom, we have undertaken important steps towards building a microscopic dynamic nuclear model. The Milano group has traditionally worked on the idea via the implementation of the so-called particle vibration coupling (PVC) model [32–34], yet different physical and technical difficulties need to be faced [35–38]. One of the most important drawbacks is the correct treatment of the renormalization of the interaction. By renormalization, we mean curing the divergences whenever they appear due to the nature of the effective interaction employed and/or consistently determining the renormalized parameters with the adopted many-body scheme.

In more detail, one can solve the nuclear effective Hamiltonian using perturbation theory up to the first order (Hartree–Fock) and find a static solution where the nuclear field is just an average static field. The consequence is that nucleons are predicted to be frozen in their quantum states, and single-particle dynamics are, thus, not realistic. To solve this problem one needs, for example, to go beyond the Hartree–Fock approximation, that is, up to higher orders in perturbation theory [39]. If summing up some specific types of diagrams—those which are supposed to provide the largest contributions—that correspond to collective low-energy vibrations, one can recover, ultimately, a PVC model. Our recent efforts to understand the renormalization problem lay on the basis of a simplified model that corresponded to the lowest-order approximation on the perturbation series expansion of a microscopic PVC approach [35–38]. In other words, we aim at building a PVC model in a more systematic way

[5] The Nobel Prize in Physics 1975 was awarded jointly to Aage Niels Bohr, Ben Roy Mottelson and Leo James Rainwater 'for the discovery of the connection between collective motion and particle motion in atomic nuclei and the development of the theory of the structure of the atomic nucleus based on this connection' https://nobelprize.org/nobel_prizes/physics/laureates/1975/

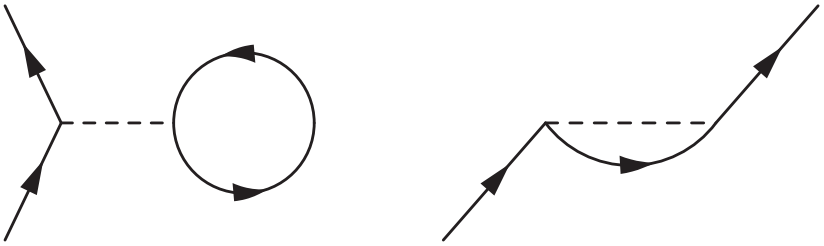

Figure 1. Diagrammatic representation for the HF self-energy. On the left the direct term $\langle 12|V|12\rangle$ is shown, and on the right the exchange term $\langle 12|V|21\rangle$.

than those adopted so far, making it possible for us to treat the renormalization of the interaction vertices at all levels formally and reliably.

Existing implementations of the PVC approach, based on relativistic and non-relativistic frameworks, are available in the literature [29, 33, 39–45]. The PVC approach has been shown to describe to a good extent the width of giant resonances, not satisfactorily explained within the TDHF, LRT or RPA. This feature is crucial for reliably estimating the beta-decay half-life of a nucleus [46] or the branching ratios for γ [47] or neutron decays [34]. It also allows the dependence of the effective mass with energy and momentum to be estimated [48], or in other words, for a more realistic optical potential [49, 50], which is the essential ingredient in any nuclear reaction calculation. Based on such a successful experience, it is timely to continue the efforts of our group, in which both single-particle and vibrational (phonon) degrees of freedom are taken into account and consistently calculated within the same microscopic interaction, by overcoming the difficulties relating to renormalization.

Our strategy is to work on different fronts in order to tackle the different problems in both the nuclear effective interactions used and the many-body techniques employed. As mentioned, one important issue that needs to be understood and solved is the renormalization of the effective interaction in approximations beyond EDFs (BEDFs). In this contribution we will implement the so-called subtraction method[6] [52, 53] to our PVC model for the first time. Such a method has previously been introduced by other groups [45, 54–56] in order to avoid double counting when going to BEDF. However, it has not yet been demonstrated whether such a procedure properly renormalizes the theory.

Finally, it is important to mention that all these studies perfectly complement the experimental activities in our group [57, 58] and worldwide. With the advent of new rare ion beam facilities [59], the experimental investigation of proton- and neutron-rich unstable nuclei has become possible. Nuclear theory should cover and provide reliable predictions for the properties of this unexplored area of the nuclear chart, not to mention the relevance of a deep understanding of the structure of new super-heavy elements [60, 61].

2. Formalism

In this section, we will briefly describe the basis of our formalism paying attention to underlying physical assumptions and referring the reader to the references herein for technical details.

[6] The subtraction method has been devised as a way of extending the stability condition of RPA equations to theories beyond such an approach, e.g. the second RPA (SRPA) [51].

Figure 2. A diagrammatic representation of the infinite series of the RPA approximation. The infinite sum of bubbles represents a vibration or a phonon state.

In general, the nuclear Hamiltonian can be written as $\mathcal{H} = T + V$, where T represents the kinetic energy, and V the two-body and three-body—or density dependent two-body—effective interaction between nucleons. Adding and subtracting an auxiliary one-body potential U allows us to formulate the problem in terms of a noninteracting part $\mathcal{H}_0 \equiv T + U$ that corresponds to the so-called HF Hamiltonian if the auxiliary potential is defined as the ground state expectation value of V on a Slater determinant, plus $V-U$, which vanishes by construction within the HF approximation. That is, the solution of $\mathcal{H}_0$ coincides with that of $\mathcal{H}$ in first order perturbation theory. The diagrammatic representation for the HF self-energy can be seen in figure 1. In what follows, we will denote as $|i\rangle$ the set of occupied and unoccupied HF states with energy ε_i.

Considering $V-U$ in higher order perturbation theory, that is, adopting the unperturbed Hamiltonian as $\mathcal{H}_0$, the contribution of U will be exactly zero in all cases[7]. Hence, standard perturbation theory techniques can be applied directly to the potential V for higher order calculations. However, to apply such a strategy is very complicated from a technical point of view, and the implementation of higher order contributions may not entail, in general, a clear physical interpretation. Alternatively, one may select the most relevant diagrams that should play a clear physical role and sum them up to infinite order, if possible. Hence, it is crucial to understand the relevant degrees of freedom of the problem under consideration and to connect them with given terms in the many-body expansion. This is the case of the vibrational degrees of freedom or phonons in nuclei[8]. When coupled to single-particle degrees of freedom, collective low-energy nuclear vibrations constitute one of the major actors in generating the fragmentation of the latter, giving rise to the so-called spreading width observed in nuclei. At larger energies, the collective motion in nuclei gives rise to a prominent dynamic effect: giant resonances [12, 30, 62]. These are the super-positions of particle–hole excitations. In particular, phonons are built from a very specific type of diagram summed up to infinity, which corresponds to solve the RPA equations. Such a series of diagrams, including a particle (unoccupied state) hole (occupied state) excitation (1p–1h), named a bubble diagram, is represented in figure 2.

Therefore, it is customary to work within a subspace $\mathcal{Q}_1$ that contains all the nuclear 1p–1h configurations built with the single-particle states $|i\rangle$, which are the eigenfunctions of the HF Hamiltonian, where the RPA—in a discrete space in our case—will correspond to solve the initial Hamiltonian projected in the $\mathcal{Q}_1$ subspace $\mathcal{Q}_1\mathcal{H}\mathcal{Q}_1$. The RPA states built in this way are linear combinations of 1p–1h (HF) states, which represent, as mentioned, a nuclear vibration or phonon. A discretized RPA calculation may display the spread of different

[7] This is because in perturbation theory, the matrix elements of $V-U$ appearing in higher order contributions to the energy or wave function can always be written in terms of the unperturbed bases.
[8] Rotational degrees of freedom also play an important role, but we will not discuss this here.

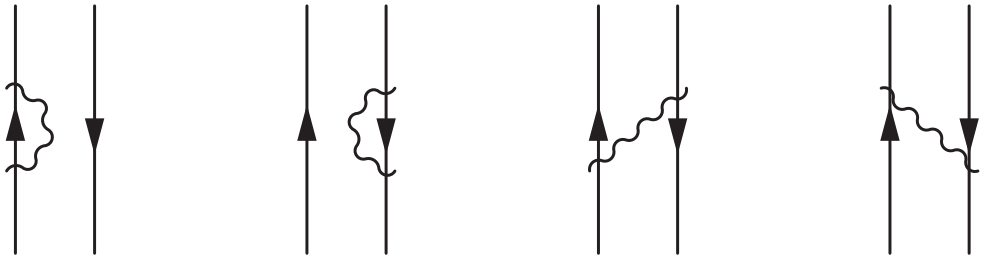

Figure 3. A diagrammatic representation of the terms contributing to the spreading width in the PVC approach.

excitation peaks producing a broadening of the giant resonance in contrast with the ideal situation, in which there is a clear single and collective peak. Such an effect depends on the intensity of the residual interaction that particle–hole configurations feel, as well as the density of the unperturbed 1p–1h states around a given excitation energy. This effect is well known in the literature and it is named Landau damping. In addition, it is worth mentioning that if the continuum is discretized, the RPA states are stationary states with no spreading width. The reason for this is that the RPA does not introduce an energy dependence in the self-energy.

In general, the coupling of nuclear vibrational states with single-particle states[9] permits the transfer of energy from one degree of freedom to another. This allows for the rearrangement of the internal degrees of freedom, giving rise to damping via the so-called spreading width ($\Gamma^{\downarrow}$). A PVC approach also provides a more realistic description—when compared to the HF or RPA results—of the emission of a γ ray and the escape of nucleons, which contributes to the so-called escape width ($\Gamma^{\uparrow}$). In figure 3 we show the diagrammatic representation of the terms contributing to the spreading width in the PVC approach.

As in [34], in order to model the escape and spreading widths, we define two additional subspaces. The first one $\mathcal{P}$ is made of holes plus unbound HF states which have positive energy, and which we construct to be orthogonal to the bound occupied and unoccupied HF states $|i\rangle$ by solving $\mathcal{H}_0$ for those additional scattering states labeled as $|s\rangle$. The second subspace $\mathcal{Q}_2$ is made of 1p–1h excitations $|ph\rangle$ coupled to a phonon state labeled as $|N\rangle$. Note that by construction $\mathcal{Q}_1\mathcal{Q}_2 = 0$ since $\langle ph|N \otimes ph\rangle$ will always be zero. Finally, we define the subspace $\mathcal{Q} = \mathcal{Q}_1 + \mathcal{Q}_2$. The projectors $\mathcal{Q}$ and $\mathcal{P}$ cover the full model space: $\mathcal{Q} + \mathcal{P} = 1$ and $\mathcal{Q}\mathcal{P} = 0$; and all the projectors fulfill the usual conditions: $\mathcal{P}^2 = \mathcal{P}$, $\mathcal{Q}^2 = \mathcal{Q}$ and $\mathcal{Q}_i^2 = \mathcal{Q}_i$.

The Green's function formalism gives a natural representation of the response of a quantum mechanical system to a given perturbation. The dynamical many-body Green's function $\mathcal{G}$ of an interacting system described by a Hamiltonian $\mathcal{H}$ evaluated at a given energy ω, is a solution of the operator equation

$$(\omega - \mathcal{H} - i\epsilon)\mathcal{G}(\omega) = 1. \tag{1}$$

Within our model, the Green's function $\mathcal{G}(\omega)$ can be split into different terms using the defined subspaces as

[9] For consistency within the adopted many-body scheme, it is important to note that when coupling a phonon state with a particle state, the one-bubble diagram has to be subtracted from the self-energy [39] (see figure 2 of the same reference). The reason for this is that the RPA phonon contains the contribution of the one-bubble diagram. Such a diagram has two equivalent fermionic lines and, thus, for symmetry reasons a factor of a half has to be taken into account. A way of implementing this symmetry is just by subtracting the one-bubble diagram. The latter considerations do not apply for higher order bubble diagrams.

$$\mathcal{G} = \mathcal{Q}\mathcal{G}\mathcal{Q} + \mathcal{Q}\mathcal{G}\mathcal{P} + \mathcal{P}\mathcal{G}\mathcal{Q} + \mathcal{P}\mathcal{G}\mathcal{P}. \tag{2}$$

Our interest is in providing a microscopic and realistic description of the dynamics in the nuclei. We therefore choose to project the Hamiltonian in the $\mathcal{Q}_1$ subspace taking into account the effects of the continuum $\mathcal{P}$ and of the more complex configurations $\mathcal{Q}_2$ in an approximate way.

Using the properties of the subspaces defined here, and following a method very similar to that in [63], we manipulate equation (1) by first sandwiching it with $\mathcal{Q}_1$,

$$\mathcal{Q}_1(\omega - \mathcal{H} - i\epsilon)\,\mathcal{Q}_1 \cdot \mathcal{Q}_1\mathcal{G}\mathcal{Q}_1 + \mathcal{Q}_1\mathcal{H}\mathcal{Q}_2 \cdot \mathcal{Q}_2\mathcal{G}\mathcal{Q}_1 + \mathcal{Q}_1\mathcal{H}\mathcal{P} \cdot \mathcal{P}\mathcal{G}\mathcal{Q}_1 = \mathcal{Q}_1; \tag{3}$$

then, similarly, we sandwich it with $\mathcal{P}$ from the left and $\mathcal{Q}_1$ from the right and, finally, with $\mathcal{Q}_2$ from the left and $\mathcal{Q}_1$ from the right. From the last two equations, analogous to equation (3), we find an expression for $\mathcal{Q}_2\mathcal{G}\mathcal{Q}_1$ and $\mathcal{P}\mathcal{G}\mathcal{Q}_1$ in terms of $\mathcal{Q}_1\mathcal{G}\mathcal{Q}_1$ that we insert into equation (3). Putting all that together one arrives at the expression,

$$(\omega - \mathcal{H}_{\mathcal{Q}_1} - i\epsilon)\,\mathcal{Q}_1\mathcal{G}(\omega)\,\mathcal{Q}_1 = \mathcal{Q}_1, \tag{4}$$

where $\mathcal{H}$ projected in the $\mathcal{Q}_1$ subspace is (see appendix)

$$\begin{aligned}
\mathcal{H}_{\mathcal{Q}_1} = {} & \mathcal{Q}_1\mathcal{H}\mathcal{Q}_1 + \mathcal{Q}_1\mathcal{H}\mathcal{P}\frac{1}{\mathcal{P}(\omega - \mathcal{H} - i\epsilon)\mathcal{P}}\mathcal{P}\mathcal{H}\mathcal{Q}_1 \\
& + \mathcal{Q}_1\mathcal{H}\mathcal{Q}_2\frac{1}{\mathcal{Q}_2(\omega - \mathcal{H} - i\epsilon)\,\mathcal{Q}_2}\mathcal{Q}_2\mathcal{H}\mathcal{Q}_1 \\
& + \mathcal{Q}_1\mathcal{H}\mathcal{P}\frac{1}{\mathcal{P}(\omega - \mathcal{H} - i\epsilon)\mathcal{P}}\mathcal{P}\mathcal{H}\mathcal{Q}_2\frac{1}{\mathcal{Q}_2(\omega - \mathcal{H} - i\epsilon)\,\mathcal{Q}_2}\mathcal{Q}_2\mathcal{H}\mathcal{Q}_1 \\
& + \mathcal{Q}_1\mathcal{H}\mathcal{Q}_2\frac{1}{\mathcal{Q}_2(\omega - \mathcal{H} - i\epsilon)\,\mathcal{Q}_2}\mathcal{Q}_2\mathcal{H}\mathcal{P}\frac{1}{\mathcal{P}(\omega - \mathcal{H} - i\epsilon)\mathcal{P}}\mathcal{P}\mathcal{H}\mathcal{Q}_1 \\
& + \text{higher order terms.}
\end{aligned} \tag{5}$$

Assuming that the continuum states are unaffected by the collective vibrations $\mathcal{P}\mathcal{H}\mathcal{Q}_2 = \mathcal{Q}_2\mathcal{H}\mathcal{P} = 0$ (see also appendix), one will recover the expression in equation (24) of [63]. Such an approximation is justified as follows. The matrix elements of $\mathcal{P}V\mathcal{Q}$ are expected to be very small due to the short range of the interaction: the overlapping between the continuum states and bound states or phonon states will occur in the space regions where the former wave functions are small. Therefore, $\mathcal{P}\mathcal{H}\mathcal{Q} \approx \mathcal{P}\mathcal{H}_0\mathcal{Q}$ where $\mathcal{P}\mathcal{H}_0\mathcal{Q}_2 = 0$ by construction. In equation (5), the first term on the right-hand side of the equation corresponds to the RPA solution, $\mathcal{Q}_1\mathcal{H}\mathcal{Q}_1$; the second term corresponds to the excitation of a bound particle or a hole state to the continuum, its propagation on top of the noninteracting (HF) potential for states with positive energy and its de-excitation to a bound state again. This term, commonly labeled as $\mathcal{W}^{\uparrow}$, will produce the escape width previously discussed. The fourth term corresponds to the coupling of a particle or hole state with more complex configurations represented by $\mathcal{Q}_2$, its propagation on top of the potential and the reabsorption of this complex state into a particle or a hole. This term, commonly labeled as $\mathcal{W}^{\downarrow}$, will produce the spreading width previously discussed. The last two terms are higher order contributions to $\mathcal{W}^{\uparrow}$ and $\mathcal{W}^{\downarrow}$, which account for the effects of nuclear vibrations in continuum states. These terms are neglected in our calculations for the reasons discussed above.

Hence, we define within our approximations,

$$\mathcal{W}^{\uparrow}(\omega) \equiv \mathcal{Q}_1\mathcal{H}\mathcal{P}\frac{1}{\mathcal{P}(\omega - \mathcal{H} - i\epsilon)\mathcal{P}}\mathcal{P}\mathcal{H}\mathcal{Q}_1 \tag{6}$$

$$\mathcal{W}^{\downarrow}(\omega) \equiv \mathcal{Q}_1\mathcal{H}\mathcal{Q}_2\frac{1}{\mathcal{Q}_2(\omega - \mathcal{H} - i\epsilon)\mathcal{Q}_2}\mathcal{Q}_2\mathcal{H}\mathcal{Q}_1. \tag{7}$$

For the escape term, within our previous approximations, one can take advantage of $\mathcal{Q}\mathcal{H}\mathcal{P} \approx \mathcal{Q}\mathcal{H}_0\mathcal{P}$ and consistently employ the Green's function solution of $(\omega - \mathcal{H}_0 - \mathrm{i}\epsilon)\mathcal{G}_0 = 1$. Therefore, similar to equation (29) of [63], one can write it as

$$\begin{aligned}\mathcal{W}^{\uparrow}(\omega) &= \mathcal{Q}_1(\omega - \mathcal{H}_0 - i\epsilon)\,\mathcal{Q}_1 - \frac{1}{\mathcal{Q}_1\mathcal{G}_0\mathcal{Q}_1} \\ &= \omega - \mathcal{Q}_1\mathcal{H}_0\mathcal{Q}_1 - \frac{1}{\mathcal{Q}_1\mathcal{G}_0\mathcal{Q}_1}.\end{aligned} \tag{8}$$

Provided a sufficiently large basis $|i\rangle$ is employed, the accuracy of this procedure is comparable to the exact continuum RPA calculations [64].

In what follows, we define some useful and related quantities. The observed spectrum of a nucleus excited by an external field $\mathcal{F}$ is described by the nuclear polarization propagator or dynamic polarizability $\Pi(\omega)$. This corresponds to the double convolution with $\mathcal{F}$ of the propagator or response function, i.e. in our specific case $\mathcal{G}_{\mathcal{Q}_1}(\omega) \equiv \mathcal{Q}_1\mathcal{G}(\omega)\,\mathcal{Q}_1 = (\omega - \mathcal{H}_{\mathcal{Q}_1}(\omega) + i\epsilon)^{-1}$, that is

$$\Pi(\omega) = \langle 0|\mathcal{F}^{\dagger}\frac{1}{\omega - \mathcal{H}_{\mathcal{Q}_1}(\omega) + i\epsilon}\mathcal{F}|0\rangle. \tag{9}$$

The strength function is defined as

$$\mathcal{S}(\omega) = -\frac{1}{\pi}\Im[\Pi(\omega)]. \tag{10}$$

Finally, some of the moments of the strength function are of special interest, since they are subject to the fulfilling of some existing sum rules. The k-moment of the strength function is defined as

$$m_k = \int_0^{\infty} \omega^k \mathcal{S}(\omega)\mathrm{d}\omega, \tag{11}$$

where m_0 corresponds to the so-called non-energy weighted sum rule (NEWSR), m_1 corresponds to the so-called energy weighted sum rule (EWSR) and m_{-1} to the inverse energy weighted sum rule (IEWSR). The latter is proportional to the static limit of the dynamic polarizability $\Pi(\omega = 0) = -2m_{-1}$.

2.1. The subtraction method

Commonly in nuclear physics, the determination of EDF parameters is done at the H or HF levels as previously explained. Obviously, effective theories that go beyond the H or HF approaches should be refitted to the experimental data in order to avoid double-counting. That is, a renormalization of the model parameters is compulsory with respect to those determined within the H or HF approaches. The parameters will change their value since physical many-body terms beyond the H or HF approximations are now explicitly included. The purpose of the subtraction method [52, 53] is to provide a recipe for the renormalization of the effective interaction within the adopted model scheme that avoids a refitting of the parameters. We will see that such a method is suitable for renormalizing the expectation value of one-body operators only. Therefore, whether this is equal to a refit of the interaction, or a proper way to do so, is a question that would depend on the nature of the studied (fitted) observables. Another related but different issue is the renormalization of the divergences that appear in

BEDF theories when zero-range effective interactions are adopted (see for example [35, 37] and section 2.3 below).

Apart from the renormalization of the interaction, the subtraction method proposed in [53] has been devised to keep the stability condition of an RPA-like matrix when going beyond the RPA. This should be one of the most important points for justifying such a procedure. The stability condition guarantees real eigenvalues and implies that the Slater determinant on which the RPA-like matrices are based must be a minimum of the energy. In this regard, we note that our theoretical method allows us to write the equations to be solved as an energy-dependent RPA-like matrix (see equation (2.5) in [34]).

In what follows, we review the underlying idea of the subtraction method. For technical details we refer the reader to the original reference [53]. In general, the dynamic polarizability $\Pi(\omega)$ follows the equation

$$\Pi(\omega) = \Pi_0(\omega) + \Pi_0(\omega) W(\omega) \Pi(\omega) \tag{12}$$

where $W(\omega)$ represents, in general, an induced effective interaction, and $\Pi_0(\omega)$ the dynamic polarizability at the level of approximation that one wants to improve. That is, if the RPA approach is adopted (see figure 2), $\Pi_0 = \Pi_{\rm HF}$ and W is the so called particle–hole (or residual) interaction that is defined as

$$W_{\rm RPA}(1,\,2) \equiv \frac{\delta^2 E[\rho]}{\delta\rho_1 \delta\rho_2} \tag{13}$$

where $E[\rho]$ represents the EDF of choice.

Now, assuming that we are dealing with the exact nuclear EDF $E[\rho]$, and that it can be derived from a Hamiltonian, DFT ensures that $E[\rho;\,\lambda] = E[\rho] + \lambda\mathcal{O}$ will also describe the ground state of the perturbed system exactly if $\mathcal{O}$ is a one-body operator. Such an observation implies that the expectation value of any one-body operator calculated using the ground-state wave function solution of the constrained calculation, i.e. the solution of $\tilde{\mathcal{H}} = \mathcal{H} + \lambda\mathcal{O}$, is also exact. Via the dielectric theorem [65], which establishes that $m_{-1} = \frac{1}{2}\partial^2_\lambda \langle\lambda|\mathcal{H}|\lambda\rangle|_{\lambda=0}$, one should conclude that m_{-1} should be conserved in the BEDF calculations, as compared to its value calculated within the exact EDF. In this case, it is shown that m_{-1} should be conserved, but it might be that other features related to the response function require the same treatment.

One of the possible realizations that conserve the value of m_{-1} in BEDF approaches is as suggested in [53]. In this reference, it is shown that recovering the static limit of the dynamic polarizability is the equivalent of recovering the RPA response function $\mathcal{G}_{\rm RPA}$ in the BEDF approaches. This would imply, in practice, the modification of equation (12) as follows:

$$\Pi_{\rm BEDF}(\omega) = \Pi_{\rm RPA} + \Pi_{\rm RPA}[W_{\rm BEDF}(\omega) - W_{\rm BEDF}(\omega = 0)]\Pi(\omega)_{\rm BEDF} \tag{14}$$

since it is now ensured that $\Pi_{\rm BEDF}(\omega = 0) = \Pi_{\rm RPA}$ and, therefore, $\mathcal{G}_{\rm BEDF}(\omega = 0) = \mathcal{G}_{\rm RPA}$ (see equation (9)). In our specific case, the induced effective interaction will be $W_{\rm PVC}(\omega) \equiv \mathcal{W}^{\uparrow}(\omega) + \mathcal{W}^{\downarrow}(\omega) - \mathcal{W}^{\downarrow}(\omega = 0)$.

Hence, the subtraction method directly impacts on many properties of the excited modes in the nuclei, although it should restore the EDF values for the expectation value of the one-body operators due to the redefinition (renormalization) of $W(\omega)$. Therefore, studying how such a method performs in practice, for those cases in which we know that the result should be conserved in the BEDF calculations with respect to the EDF calculations, is of prominent importance.

2.2. Sum rules

Thouless theorem [66] states that the EWSR calculated within the RPA approach is equal to the HF expectation value of the double commutator $\frac{1}{2}[\mathcal{F}, [\mathcal{H}, \mathcal{F}^\dagger]]$, where $\mathcal{F}$ represents the external field that perturbs the nuclear ground state. In [67] it was proven that the EWSR in the second RPA (SRPA) [51, 68] is also equal to the double commutator calculated within the HF ground state and, therefore, also to the RPA value. Such a result was derived without implementing the subtraction method. Actually, this proof is valid for both the full SRPA, and the SRPA calculations where the 2p–2h subspace has been eliminated by introducing an energy-dependent effective interaction in the 1p–1h subspace [68] (see below). As a matter of fact, the RPA, as well as the latter proof, are based on the quasiboson approximation, where the expectation value of the operators is calculated within the uncorrelated HF ground state, instead of a more consistent treatment, which would consider the correlated RPA (or SRPA) ground state [69]. In this regard, the subtraction method should provide a correlated wave function for the ground state that should give the same results, when applied to the calculation of the expectation value of any one-body operator, as the HF expectation value of the same operator. This is because of the redefinition of the induced effective interaction in the static limit ($\omega = 0$). Due to these considerations, when the result of the double commutator $[\mathcal{F}, [\mathcal{H}, \mathcal{F}^\dagger]]$ is a one-body operator, the EWSR calculated within the SRPA method—and possibly also the PVC method—with and without subtraction should not differ much in practice from the RPA result.

Regarding the IEWSR or static polarizability $\Pi(\omega = 0) = -2m_{-1}$: from [68] it is easy to understand the amount by which W should be corrected in SRPA to recover the same value for the IEWSR found in RPA (see equation (2.87)); it actually coincides with the subtraction method of [53]. An easy way to see this is as follows. Starting from the (full) SRPA matrix (see for example equation (2.48) in [68]) where the 1p–1h and 2p–2h terms are assumed to interact, one can easily rearrange the rows and columns such that the resulting matrix separates within different subspaces that enclose the 1p–1h ($\mathcal{Q}_1$) and 2p–2h ($\mathcal{Q}'_2$) subspaces separated in blocks along the diagonal, while outside the diagonal the interaction terms appear between both subspaces. By using the technique described above [63], one may project the original Hamiltonian $\mathcal{H}$ into the $\mathcal{Q}_1$ subspace, taking into account the effects of the $\mathcal{Q}'_2$ subspace perturbatively. For this, the only assumption is to neglect the residual interaction in the $\mathcal{Q}'_2$ subspace. Having done that, the induced effective interaction can be modified by an energy dependent term

$$W_{\rm SRPA}(\omega) = W_{\rm RPA} + \mathcal{Q}_1\mathcal{H}\mathcal{Q}'_2\frac{1}{\mathcal{Q}'_2(\omega - \mathcal{H} - i\epsilon)\mathcal{Q}'_2}\mathcal{Q}'_2\mathcal{H}\mathcal{Q}_1. \tag{15}$$

The latter correction written within the standard SRPA matrix formulation can be seen in equation (2.69) of [68]. By inspecting now the expression for m_{-1} in SRPA (see also equation (2.87) of [68]) and imposing that m_{-1}(SRPA) = m_{-1}(RPA), or equivalently $\Pi_{\rm SRPA}(\omega = 0) = \Pi_{\rm RPA}$, one easily realizes from equation (9) that there is an extra term that one will need to subtract in order to fulfill the latter equality. Such a term actually coincides with the one proposed by the subtraction method. Therefore, for sufficiently weak perturbations, the energy-dependent SRPA reduction from the full SRPA should be accurate, and the subtraction method proposed by Tselyaev [53] should properly work and conserve the value of the static polarizability in such an extension BEDF.

We will now analyze m_1 and m_{-1} from a different perspective. Consider that the ground state density is perturbed by an external (one-body) field $\lambda\mathcal{F}$. Changes in the expectation value of the Hamiltonian $\mathcal{H}$ can be written as,

$$\delta\langle\mathcal{H}\rangle_{\mathcal{F}} = \lambda^2 \sum_{n\neq 0} \frac{|\langle n|\mathcal{F}|0\rangle|^2}{E_n} + \mathcal{O}(\lambda^3) = \lambda^2 m_{-1} + \mathcal{O}(\lambda^3) \tag{16}$$

where standard perturbation theory has been applied (i.e. $|n\rangle$ and E_n represent an excited state and the corresponding energy of the system). In other terms,

$$m_{-1} = \frac{1}{2}\frac{\partial^2\langle\mathcal{H}\rangle_{\mathcal{F}}}{\partial\lambda^2}\bigg|_{\lambda=0} \tag{17}$$

which is nothing but the dielectric theorem [65] previously introduced. If we consider the case in which $\mathcal{F}$ is an isoscalar and velocity-independent operator and define the operator $\tilde{\mathcal{F}} \equiv i[\mathcal{H}, \mathcal{F}] = i[T, \mathcal{F}]$ where T is the kinetic energy, we can calculate the change in the expectation value of the Hamiltonian when perturbed by $\tilde{\mathcal{F}}$ and find

$$\delta\langle\mathcal{H}\rangle_{\tilde{\mathcal{F}}} = \lambda^2 \sum_{n\neq 0} E_n |\langle n|\mathcal{F}|0\rangle|^2 + \mathcal{O}(\lambda^3) = \lambda^2 m_1 + \mathcal{O}(\lambda^3). \tag{18}$$

This observation [65] allows one to state that for some specific operators (excitation modes) the Thouless theorem for $\mathcal{F}$ is equivalent to the dielectric theorem applied to $\tilde{\mathcal{F}}$,

$$m_1 = \frac{1}{2}\frac{\partial^2\langle\mathcal{H}\rangle_{\tilde{\mathcal{F}}}}{\partial\lambda^2}\bigg|_{\lambda=0} = \frac{1}{2}\langle 0|[\mathcal{F}, [\mathcal{H}, \mathcal{F}]]|0\rangle, \tag{19}$$

provided that the corresponding quantities are calculated consistently within the same approximation. Hence, we see again that whenever $\langle 0|[\mathcal{F}, [\mathcal{H}, \mathcal{F}]]|0\rangle_{\mathrm{BEDF}} \approx \langle 0|[\mathcal{F}, [\mathcal{H}, \mathcal{F}]]|0\rangle_{\mathrm{HF}}$, the EWSR of some special excitation modes should be conserved when going to BEDF.

As a final remark, it has also been shown in [68] that the NEWSR m_0 within the SRPA approach coincides with the same quantity calculated within the RPA approach whenever a subtraction is not implemented. To check this feature together with the results for the m_1 and m_{-1} within the PVC approach might shed some light onto the connection between the sum rules calculated at different levels of approximation in the adopted many-body scheme, and on the renormalization of the particle-vibration approach.

2.3. Ultraviolet divergences

So far, the considerations here do not take into account the renormalization of the ultraviolet divergences arising from the BEDF models, if based on zero-range effective interactions [35], such as the widely used Skyrme as well as part of the Gogny interaction [70], or the so-called point-coupling relativistic models [71]. Interestingly, ultraviolet divergences seem to be avoided by the subtraction method. Hence, in this context, this method can be regarded as a practical recipe that should be employed with caution, since it is yet to be demonstrated that it properly renormalizes the theory. The reabsortion of the ultraviolet divergence by the subtraction method is as follows. In general, one can write in second order perturbation theory

$$W(\omega; 1, 2) - W(\omega = 0; 1, 2) = \sum_n \frac{\langle 1|V|n\rangle\langle n|V|2\rangle}{\omega - \omega_n} + \sum_n \frac{\langle 1|V|n\rangle\langle n|V|2\rangle}{\omega_n} \tag{20}$$

where 1 and 2 indicate two different nuclear states and n is the complete basis of the nuclear intermediate states that connect the initial and final states via the effective interaction V. As evident from the last equation, for $\omega_n \to \infty$ the divergence is canceled.

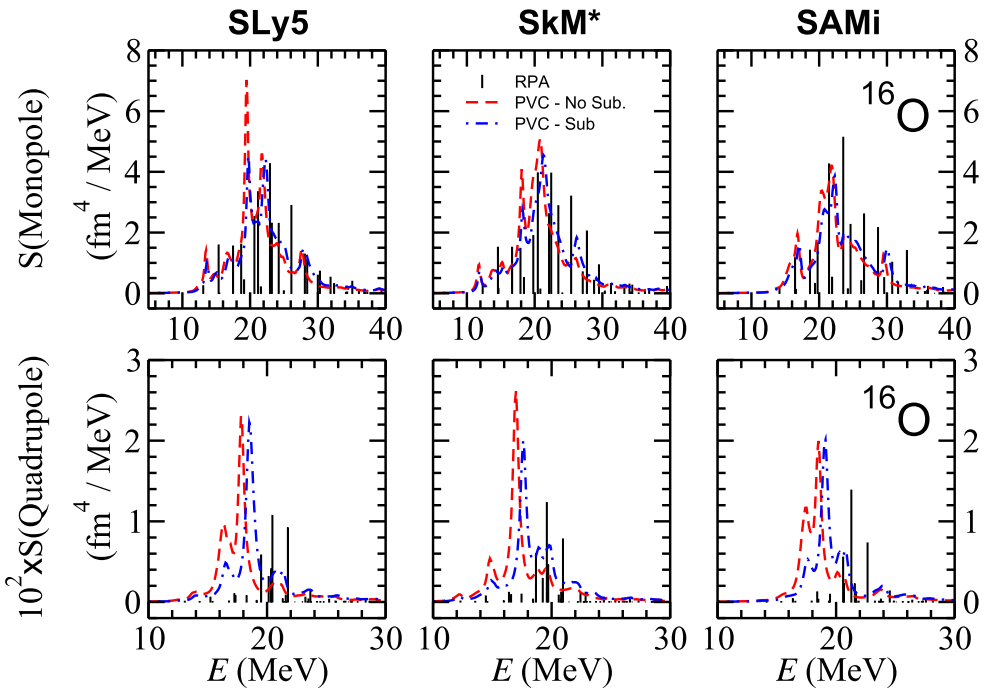

Figure 4. The results for the monopole (upper panels) and quadrupole (lower panels) response in ^{16}O as predicted by three Skyrme interactions: SLy5 [72] (left panels), SkM* [73] (middle panels) and SAMi [3] (right panels). The RPA response is depicted in black bars. The PVC results without subtraction are shown in dashed red lines and with subtraction in dashed-pointed blue lines.

3. Results

As discussed, one of the important test grounds for the subtraction method is the analysis of some specific sum rules. With the questions raised in the previous section in mind, we will study the m_0 (NEWSR), m_1 (EWSR), m_{-1} (IEWSR) and the centroid energies m_1/m_0 and $\sqrt{m_1/m_{-1}}$ for the isoscalar monopole $\mathcal{F}_0^{\rm IS} = \sum_{i=1}^{A} r_i^2 Y_{00}(\hat{r}_i)$ and quadrupole $\mathcal{F}_2^{\rm IS} = \sum_M \sum_{i=1}^{A} r_i^2 Y_{2M}(\hat{r}_i)$ modes of excitation in the test case of ^{16}O. This will be in analogy with [55], where the same cases have been studied within the SRPA approach. The selection of these one-body, isoscalar and velocity independent external fields is motivated by the discussions made in the previous section in connection with the calculation of m_1 and m_{-1}. In order to assess the systematics on our results, we have adopted three different nonrelativistic effective interactions, SLy5 [72], SkM* [73] and SAMi [3], commonly used in nuclear physics.

In addition, we will show our results for the isoscalar monopole response in ^{208}Pb due to its relevance in the determination of nuclear matter incompressibility and of the isoscalar quadrupole response in ^{208}Pb, since it is connected to the value of the effective mass at the Fermi surface. We will also comment on our results for the low-lying 2_1^+ state in ^{208}Pb, which has been argued in [56] not to be strongly affected by complex configurations such as the coupling to a phonon state.

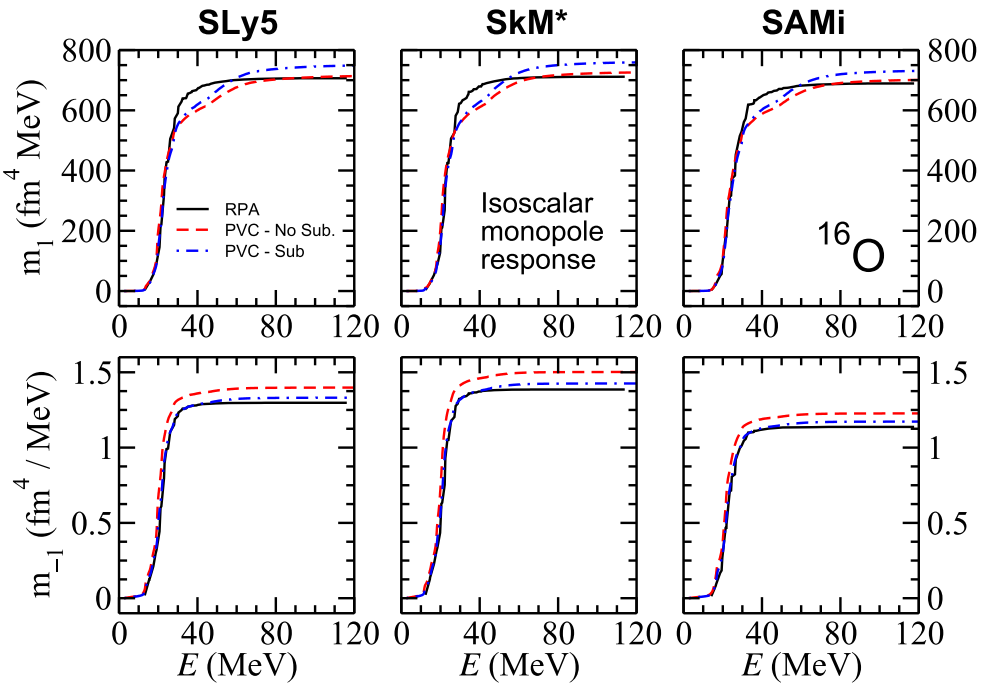

Figure 5. Cumulative sums for the EWSR (upper panels) and IEWSR (lower panels) for the monopole response in ^{16}O as predicted by three Skyrme interactions: SLy5 [72] (left panels), SkM* [73] (middle panels) and SAMi [3] (right panels). The RPA results are depicted in black lines, while the PVC results without subtraction are shown by dashed red lines and with subtraction by dashed-pointed lines.

The model space in our calculations is defined by a radial mesh of 200 points in steps of 0.1 fm and a maximum particle energy of 80 MeV. We have checked that the doorway phonons of non-natural parity are negligible for the studied cases and, thus, we only include phonons of natural parity up to multipolarity equal to 5, with an energy less than 30 MeV and absorbing a fraction of the NEWSR larger than 2%. Such a choice gives converged results for the different moments of the strength function studied here. We use a smearing parameter of 250 keV. The full effective interaction is self-consistently kept in all vertices at all the levels of approximation studied here. Our model has also been tested for the well-known Gamow–Teller resonance [43, 46], without accounting for the subtraction, and contemporary to our present work in [44] including the subtraction.

3.1. Sum rules

The EWSR for the isoscalar monopole and quadrupole responses in ^{16}O has been seen to change in the SRPA calculations with respect to the double commutator sum rule calculated at the HF level when the subtraction method is adopted (see figure 13 in [55]). In the same work, the EWSR is conserved when the subtraction is not implemented. This is in agreement with [67, 68], where it was shown that the EWSR is conserved for SRPA calculations without subtraction. As a matter of fact, the changes produced by the subtraction method on the prediction of the EWSR in the SRPA calculations presented in [55] are not very large ($\lesssim$10%).

Table 1. NEWSR (m_0) in fm^4, EWSR (m_1) in fm^4 MeV, IEWSR (m_{-1}) in fm^4/MeV and the centroid energies m_1/m_0 and $\sqrt{m_1/m_{-1}}$ in MeV for the monopole response in ^{16}O. DC stands for the double commutator sum rule calculated within the HF ground state. The percentages relating to the PVC results refer to the RPA and those of the RPA to the DC.

Force	Sum rule	DC	RPA	(%)	PVC (No Sub.)	(%)	PVC (Sub.)	(%)
SLy5	m_0		29.5		29.9	101	29.8	101
	m_1	706	707	100	713	101	749	106
	m_{-1}		1.30		1.40	108	1.33	102
	m_1/m_0		24.0		23.9	100	25.1	105
	$\sqrt{m_1/m_{-1}}$		23.3		22.6	96	23.7	100
SkM*	m_0		30.5		31.2	102	31.1	102
	m_1	712	712	100	726	102	759	107
	m_{-1}		1.39		1.50	108	1.43	103
	m_1/m_0		23.3		23.3	100	24.4	105
	$\sqrt{m_1/m_{-1}}$		22.7		22.0	97	23.1	102
SAMi	m_0		27.3		27.8	102	27.8	102
	m_1	688	689	100	701	102	731	106
	m_{-1}		1.14		1.23	108	1.17	103
	m_1/m_0		25.3		25.2	100	26.3	104
	$\sqrt{m_1/m_{-1}}$		24.6		23.9	97	25.0	102

In figure 4, we show our PVC results for the monopole (upper panels) and quadrupole (lower panels) response in ^{16}O as predicted by three Skyrme interactions: SLy5 (left panels), SkM* (middle panels) and SAMi (right panels). The RPA response is depicted in black bars, the PVC results without subtraction are shown in dashed red lines, and with subtraction in dashed-pointed blue lines. For the case of the monopole response, the PVC correlations do not affect the strength function in the giant resonance region qualitatively, and the subtraction method has consistently little impact. Such a small PVC effect is well understood from the theory (see section IV.B in [33]). The first (second) and third (fourth) diagrams, reading from the left in figure 3, correspond to the matrix elements of the type particle–particle (hole–hole) squared and particle–particle and hole–hole mixed that differ by a geometrical factor (6-j symbol, see equation (A12) in [34]). These matrix elements are essentially equal, and with an opposite sign in the case of the $L = 0$ excitation modes.

For the quadrupole response instead, we see from figure 4 that the PVC results qualitatively modify the strength function with respect to the RPA results, by producing a shift in energy of the giant resonance peak. This is because the real part of the self-energy or, equivalently, the effective mass has been strongly modified by the PVC [74]. Such a change is expected since we know that the effective mass (m^*) at the Fermi surface ($m^*/m \approx 1$ where m is the bare nucleon mass) is not well described within the EDF models ($m^*/m \approx 0.7$) and it is corrected in the right direction by the PVC approach [48]. We will come back to this point for the case of ^{208}Pb.

The differences on the predicted sum rules for the monopole case can clearly be seen in figure 5 (and table 1), where the cumulative sums for m_1 (upper panels) and m_{-1} (lower panels) are displayed, following the same color and line-type code as in figure 4. In this figure, it is clear that the EWSR is recovered within the PVC approach with no subtraction, while the PVC results with subtraction slightly overestimate m_1 by 6%–7% (see table 1). This

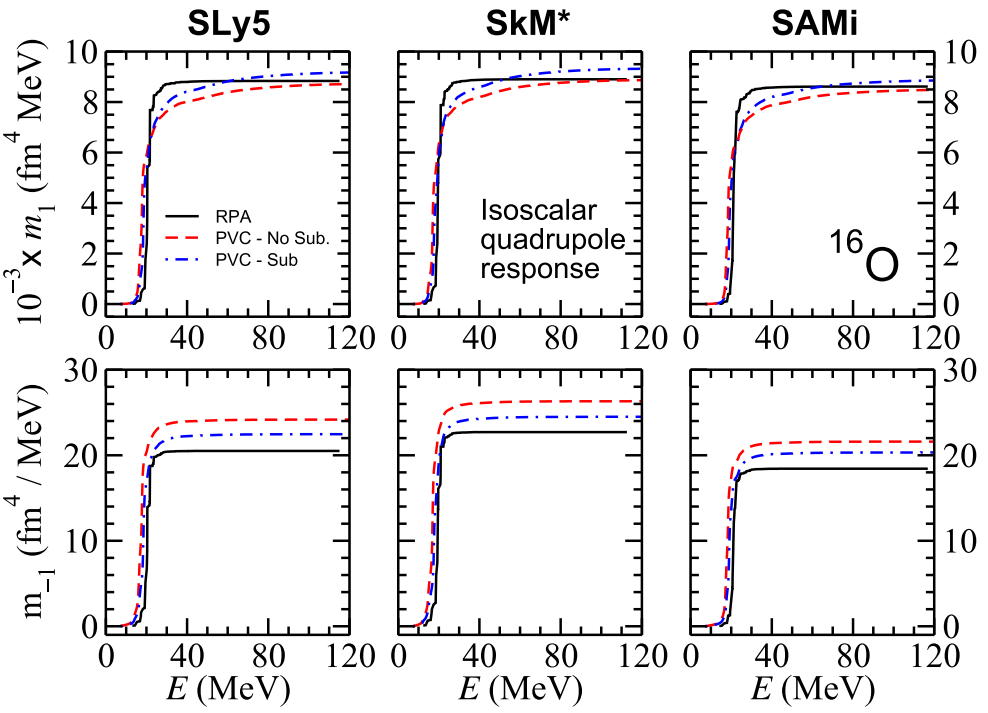

Figure 6. Cumulative sums for the EWSR (upper panels) and IEWSR (lower panels) for the quadrupole response in ^{16}O as predicted by three Skyrme interactions: SLy5 [72] (left panels), SkM* [73] (middle panels) and SAMi [3] (right panels). The RPA results are depicted in black lines, while the PVC results without subtraction are shown by dashed red lines, and with subtraction by dashed-pointed lines.

is in agreement with [67, 68]. Regarding the IEWSR, it is increased by 8% in the PVC predictions with no subtraction, while it is almost perfectly restored when the subtraction is implemented in agreement with what we expected from the previous considerations and with [53]. In table 1, the converged values for the monopole sum rules are shown. In addition to the quantitative information on these results discussed above, we also notice that our RPA results fully exhaust the double commutator sum rule; that the NEWSR in the PVC calculations with and without subtraction are (almost) equal to that of the RPA; that, consequently, the centroid energy m_1/m_0 is barely shifted by the PVC calculations without subtraction, while it is shifted upwards by about 5% (1 MeV) if the subtraction is implemented; and that, consequently, the PVC predictions for the centroid energy $\sqrt{m_1/m_{-1}}$ show the same trends, although its value is slightly closer to the RPA when the subtraction is implemented ($\lesssim$2%).

The differences in the predicted sum rules for the quadrupole case can be seen instead in figure 6 (and table 2), where the cumulative sums for m_1 (upper panels) and m_{-1} (lower panels) are displayed following the same color and line-type code as in figure 4. In this figure, it is clear that the EWSR is recovered within the PVC approach with no subtraction, while the PVC results with subtraction slightly overestimate m_1 by 3%–5% (see table 2). This is again in agreement with [67, 68] and with our previous discussions. Regarding the IEWSR, it is increased by 16%–20% in the PVC predictions with no subtraction, while it is only partially restored within 10% when subtraction is implemented. Therefore, the subtraction method in our model does not perfectly work in this case, although the correction is sizeable and in the

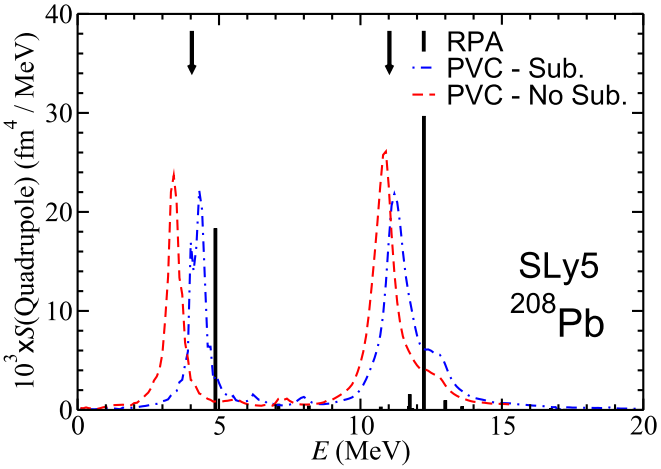

Figure 7. The isoscalar quadrupole response in ^{208}Pb as predicted by SLy5. We show the RPA response in black bars, the PVC without subtraction in dashed red lines and the PVC with subtraction in dotted-dashed blue lines. One black arrow indicates the position of the measured 2_1^+ state, and the other black arrow indicates the experimental centroid energy $m_1/m_0 = 11.0 \pm 0.2$ MeV [75].

right direction. In table 2, the converged values for the quadrupole sum rules are shown. In addition to the quantitative information on these results discussed above, we should notice that our RPA results fully exhaust the double commutator sum rule; that the NEWSR in the PVC calculations with and without subtraction are overestimated by $\lesssim$5% with respect to the RPA values; and that, consequently, the centroid energies m_1/m_0 and $\sqrt{m_1/m_{-1}}$ are barely shifted by the PVC calculations with subtraction, while they are shifted downwards by about 5%–10% ($\lesssim$2 MeV) if the subtraction is not implemented. Hence, our results are not conclusive yet, although the subtraction method gives reasonable results—within 10% accuracy—for the studied sum rules. The reason for this discrepancy is actually a measure of the accuracy of the adopted approximations, and there are essentially two: (i) the $\mathcal{Q}_2$ subspace is assumed to be made of noninteracting states; and (ii) we do not correct for the small—but present—contributions to equation (7) that violate the Pauli exclusion principle. Solving these issues should be addressed in the future.

3.2. Isoscalar quadrupole response in ^{208}Pb

Experimentally, the well-known 2_1^+ state in the low-energy isoscalar quadrupole response in ^{208}Pb is at about 4 MeV, exhausting a large fraction of the EWSR, while the giant resonance peak is at around 11 MeV and has a width of about 3 MeV [62]. The high-energy peak corresponding to the isoscalar giant quadrupole resonance is known to be related to the value of the effective mass in the vicinity of the Fermi surface ($m^*/m \sim 1$) [30]. Specifically, within a simple harmonic oscillator model, one may write that $E_x(\mathrm{ISGQR}) = \sqrt{2m/m^*}\,\hbar\omega$ where $\hbar\omega = 41A^{-1/3}$ is the shell gap. In figure 7, we show the predictions of our PVC calculations using SLy5. We show the RPA response as black bars, the PVC without subtraction in dashed red lines, and the PVC with subtraction in dotted-dashed blue lines. One black arrow indicates the position of the measured 2_1^+ state and the other black arrow indicates the experimental centroid energy $m_1/m_0 = 11.0 \pm 0.2$ MeV in the giant resonance region

Table 2. NEWSR (m_0) in fm^4, EWSR (m_1) in fm^4 MeV, IEWSR (m_{-1}) in fm^4/MeV and the centroid energies m_1/m_0 and $\sqrt{m_1/m_{-1}}$ in MeV for the quadrupole response in ^{16}O. DC stands for the double commutator sum rule calculated within the HF ground state. The percentages relating to the PVC results refer to the RPA and those of the RPA to the DC.

Force	Sum rule	DC	RPA	(%)	PVC (No Sub.)	(%)	PVC (Sub.)	(%)
SLy5	m_0		423		443	105	439	104
	m_1	8829	8836	100	8712	99	9169	104
	m_{-1}		20.50		24.17	120	22.46	110
	m_1/m_0		20.9		19.7	94	20.9	100
	$\sqrt{m_1/m_{-1}}$		20.8		19.0	91	20.2	97
SkM*	m_0		447		467	104	462	103
	m_1	8902	8902	100	8866	100	9317	105
	m_{-1}		22.71		26.31	116	24.50	108
	m_1/m_0		19.9		19.0	95	20.2	102
	$\sqrt{m_1/m_{-1}}$		19.8		18.4	93	19.5	98
SAMi	m_0		397		415	105	412	104
	m_1	8603	8612	100	8482	99	8853	103
	m_{-1}		18.43		21.60	117	20.32	110
	m_1/m_0		21.7		20.4	94	21.5	99
	$\sqrt{m_1/m_{-1}}$		21.6		19.8	92	20.9	97

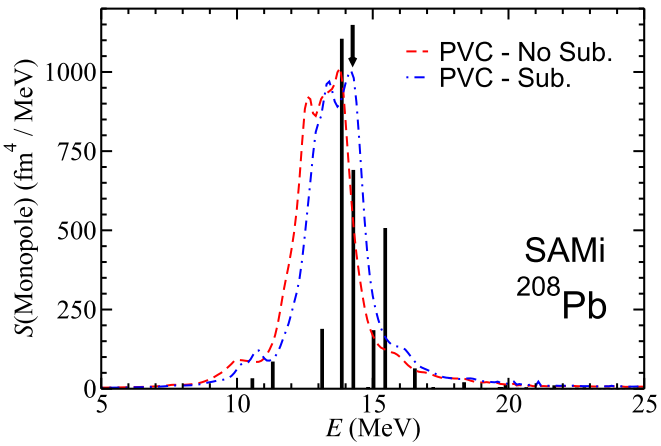

Figure 8. The isoscalar monopole response in ^{208}Pb as predicted by SAMi. We show the RPA response in black bars, the PVC without subtraction in dashed red lines and the PVC with subtraction in dotted-dashed blue lines. A black arrow indicates the centroid energy $m_1/m_0 = 14.24 \pm 0.11$ MeV measured within 8 and 22 MeV [76].

[75]. The PVC calculations show that the energy of the 2_1^+ state is affected by more complex configurations that produce a downshift in energy of about 2 MeV with respect to the RPA result when the subtraction is not implemented, and it is only slightly shifted when the subtraction is applied giving a much more realistic estimate for such a state. In this regard, our results without subtraction are not satisfactory. Regarding the giant resonance peak, as it is

well known, the RPA calculations based on the EDF with effective masses lower than the bare nucleon mass overestimate the excitation energy. As it is also well known, the PVC approach introduces an energy dependence in the real part of the self-energy that corrects the value of the effective mass [74], such that it is more realistic and compares better with the empirical value. In this regard, it seems that the results employing the subtraction method better reproduce the excitation energy of the giant resonance.

3.3. Isoscalar monopole response in ^{208}Pb

In figure 8, the isoscalar monopole response in ^{208}Pb is shown, as predicted by the SAMi interaction. We show the RPA response in black bars, while the PVC without subtraction is displayed in dashed red lines and the PVC with subtraction in dotted-dashed blue lines. A black arrow indicates the centroid energy $m_1/m_0 = 14.24 \pm 0.11$ MeV measured within 8 and 22 MeV [76]. The centroid energy defined as the square root of the ratio between the EWSR and IEWSR is $\sqrt{m_1/m_{-1}} = 14.18 \pm 0.11$ MeV [76]. The width of the resonance was measured to be between 2 and 3 MeV approximately (see table 4.1 of [62]). In our calculations using SAMi, within 8 and 22 MeV we find that for the RPA the EWSR is 97%, $m_1/m_0 = 13.7$ MeV and $\sqrt{m_1/m_{-1}} = 13.5$ MeV; for the PVC without subtraction the EWSR is 91%, $m_1/m_0 = 13.4$ MeV and $\sqrt{m_1/m_{-1}} = 13.2$ MeV; and for the PVC with subtraction the EWSR is 91%, $m_1/m_0 = 13.7$ MeV and $\sqrt{m_1/m_{-1}} = 13.6$ MeV. The width predicted by our PVC calculations is of 2 MeV. Thus, SAMi predicts reasonable values for the excitation energy and width of this resonance, both with and without subtraction, since the PVC effects are as small as expected. It is well known within the RPA approach that the excitation energy of the isoscalar giant monopole resonance and the finite nucleus incompressibility K_A can be related as follows [77]: $E_x(\mathrm{ISGMR}) \equiv \sqrt{m_1/m_{-1}} = \sqrt{\hbar^2 K_A/(m\langle r^2\rangle)}$ where $\langle r^2\rangle$ is the mean squared radius of the nucleus. Hence, our results suggest that K_A will barely be affected by PVC effects and it should then be reliably derived from the EDF models. In the limit of $A \to \infty$ one would recover the value for the nuclear matter incompressibility, which is a crucial ingredient of the nuclear equation of state that governs physical systems from the very small (the interior of a nucleus) to the very big (the interior of a neutron star).

4. Conclusions

The PVC approach presents some important points that need to be solved. In connection to this, one issue that needs to be better understood is the renormalization of the effective interaction in the particle-vibration approach. One proposed way to do this is with the so-called subtraction method [53]. This method ensures that the static limit of the dynamic polarizability is conserved in the BEDF approaches with respect to the EDF value. In addition, the subtraction method guarantees the stability condition in RPA-like theories. Both of these features are very important. As an example, the static dipole polarizability is currently being extensively theoretically studied on an EDF basis (see [19] and the references therein), and in laboratories such as the RCNP in Japan and the GSI in Germany [78–80].

In this contribution, we have implemented the subtraction method for the first time in our PVC model, and studied its suitability on the basis of existing sum rules applied as an example to the case of ^{16}O and ^{208}Pb. We have found that the subtraction method allows one to (mostly) recover the value of m_{-1} predicted at the RPA level in the PVC approach, but with some caveats: while this is almost exactly fulfilled in our calculations of the isoscalar monopole resonance in ^{16}O, it is only approximately fulfilled for the case of the isoscalar

quadrupole response in ^{16}O. These results should be further and more systematically investigated in the future. As discussed, the m_0 and m_1 moments of the strength function have also been the subject of our studies. This is because these two quantities have been shown to be conserved by the SRPA calculations with respect to their RPA counterparts when the subtraction is not implemented [67, 68]. In addition, the m_1 moment has been intensively studied down the years, both experimentally and theoretically [12, 62]. Within our calculations, the m_1 value is exactly conserved at the PVC level with respect the corresponding RPA results, only if the subtraction is not implemented and slightly overestimated otherwise.

The quantities m_1/m_0 and $\sqrt{m_1/m_{-1}}$ have been studied, since they constitute one of the possible ways of extracting the excitation energy of a given resonance. Both have been the object of many studies in the past, and their study should now be revitalized with the advent of new rare ion beam facilities that aim to measure the excitation properties in exotic nuclei. Regarding the excitation energy $\sqrt{m_1/m_{-1}}$, we have seen that our PVC calculations almost recover the RPA value when the subtraction method is applied, while it is slightly underestimated otherwise. For the centroid energy m_1/m_0, as a consequence of our previous results, we find that it is conserved for the monopole if the subtraction is not implemented and for the quadrupole if the subtraction is implemented.

We have also presented our results on the isoscalar monopole and quadrupole responses in ^{208}Pb, and learn that the finite nucleus incompressibility is barely affected by PVC effects while the effective mass—as it is well known—is properly corrected in our PVC calculations. In addition to this, we have paid special attention to the 2_1^+ state, since it has been argued [56] that it should not be strongly modified by complex configurations such as the coupling to a phonon state. We find that this is not the case when the subtraction is not implemented, since the energy of this peak is downshifted by about 2 MeV, moving far from the experimental value. We also find that it is only slightly shifted with respect to the RPA result when subtraction is applied, the latter giving a much more realistic estimate for such a state.

In summary, in all cases the moments and excitation energies agree within $\lesssim$10% with the RPA results, except for the calculation of m_{-1}, within our PVC model without implementing the subtraction. The studied giant resonances in ^{208}Pb as well as the 2_1^+ state are in reasonable agreement with the experiment by our PVC calculations if the subtraction is implemented. Our results indicate that the subtraction method renormalizes the particle-vibration approach in a good direction, although a better understanding or strategy is indeed needed in this regard. Further investigation in connection with the renormalization of the particle-vibration approach is envisaged.

Acknowledgments

YFN acknowledges partial support by the National Natural Science Foundation of China under grant no. 11305161. Funding from the European Union's Horizon 2020 research and innovation programme under grant agreement no. 654002 is acknowledged.

Appendix. Effective Hamiltonian in the $\mathcal{Q}_1$ subspace

Using the properties of the subspaces defined here, and following a method very similar to that of [63], we manipulate equation (1) by first sandwiching it with $\mathcal{Q}_1$,

$$\mathcal{Q}_1(\omega - \mathcal{H} - i\epsilon)\,\mathcal{Q}_1 \cdot \mathcal{Q}_1\mathcal{G}\mathcal{Q}_1 + \mathcal{Q}_1\mathcal{H}\mathcal{Q}_2 \cdot \mathcal{Q}_2\mathcal{G}\mathcal{Q}_1 + \mathcal{Q}_1\mathcal{H}\mathcal{P} \cdot \mathcal{P}\mathcal{G}\mathcal{Q}_1 = \mathcal{Q}_1. \tag{A.1}$$

Then, similarly, we sandwich it with $\mathcal{P}$ from the left and $\mathcal{Q}_1$ from the right and, finally, with $\mathcal{Q}_2$ from the left and $\mathcal{Q}_1$ from the right. This allows us to find the system of the operator equations:

$$\begin{pmatrix} \mathcal{P}(\omega - \mathcal{H} - i\epsilon)\mathcal{P} & -\mathcal{P}\mathcal{H}\mathcal{Q}_2 \\ -\mathcal{Q}_2\mathcal{H}\mathcal{P} & \mathcal{Q}_2(\omega - \mathcal{H} - i\epsilon)\mathcal{Q}_2 \end{pmatrix} \begin{pmatrix} \mathcal{P}\mathcal{G}\mathcal{Q}_1 \\ \mathcal{Q}_2\mathcal{G}\mathcal{Q}_1 \end{pmatrix} = \begin{pmatrix} \mathcal{P}\mathcal{H}\mathcal{Q}_1 \cdot \mathcal{Q}_1\mathcal{G}\mathcal{Q}_1 \\ \mathcal{Q}_2\mathcal{H}\mathcal{Q}_1 \cdot \mathcal{Q}_1\mathcal{G}\mathcal{Q}_1 \end{pmatrix}.$$

From this system of equations, one can find an expression for $\mathcal{Q}_2\mathcal{G}\mathcal{Q}_1$ and $\mathcal{P}\mathcal{G}\mathcal{Q}_1$ in terms of $\mathcal{Q}_1\mathcal{G}\mathcal{Q}_1$ by inverting the matrix on the left-hand side. Inserting such a solution in equation (A.1), one can find the final expression for $\mathcal{H}_{\mathcal{Q}_1}$ that fulfills

$$(\omega - \mathcal{H}_{\mathcal{Q}_1} - i\epsilon)\,\mathcal{Q}_1\mathcal{G}(\omega)\,\mathcal{Q}_1 = \mathcal{Q}_1. \tag{A.2}$$

If we assume $\mathcal{P}\mathcal{H}\mathcal{Q}_2$ and $\mathcal{Q}_2\mathcal{H}\mathcal{P}$ are negligible in the matrix on the left-hand side of the system, it is easy to invert it and find an expression for $\mathcal{P}\mathcal{G}\mathcal{Q}_1$ and $\mathcal{Q}_2\mathcal{G}\mathcal{Q}_1$ as a function of $\mathcal{Q}_1\mathcal{G}\mathcal{Q}_1$

$$\begin{pmatrix} \mathcal{P}\mathcal{G}\mathcal{Q}_1 \\ \mathcal{Q}_2\mathcal{G}\mathcal{Q}_1 \end{pmatrix} \approx \begin{pmatrix} \frac{1}{\mathcal{P}(\omega - \mathcal{H} - i\epsilon)\mathcal{P}} & 0 \\ 0 & \frac{1}{\mathcal{Q}_2(\omega - \mathcal{H} - i\epsilon)\mathcal{Q}_2} \end{pmatrix} \begin{pmatrix} \mathcal{P}\mathcal{H}\mathcal{Q}_1 \cdot \mathcal{Q}_1\mathcal{G}\mathcal{Q}_1 \\ \mathcal{Q}_2\mathcal{H}\mathcal{Q}_1 \cdot \mathcal{Q}_1\mathcal{G}\mathcal{Q}_1 \end{pmatrix}.$$

Using the latter expressions, we recover $\mathcal{H}_{\mathcal{Q}_1}$ of [63]. If we assume instead that $\mathcal{P}\mathcal{H}\mathcal{Q}_2$ and $\mathcal{Q}_2\mathcal{H}\mathcal{P}$ are small, as compared to the diagonal terms of the same matrix, we can approximately invert the matrix on the left-hand side of the equation and find

$$\begin{aligned} &\begin{pmatrix} \mathcal{P}\mathcal{G}\mathcal{Q}_1 \\ \mathcal{Q}_2\mathcal{G}\mathcal{Q}_1 \end{pmatrix} \\ &\approx \begin{pmatrix} \frac{1}{\mathcal{P}(\omega - \mathcal{H} - i\epsilon)\mathcal{P}} & \frac{1}{\mathcal{P}(\omega - \mathcal{H} - i\epsilon)\mathcal{P}}\mathcal{P}\mathcal{H}\mathcal{Q}_2\frac{1}{\mathcal{Q}_2(\omega - \mathcal{H} - i\epsilon)\mathcal{Q}_2} \\ \frac{1}{\mathcal{Q}_2(\omega - \mathcal{H} - i\epsilon)\mathcal{Q}_2}\mathcal{Q}_2\mathcal{H}\mathcal{P}\frac{1}{\mathcal{P}(\omega - \mathcal{H} - i\epsilon)\mathcal{P}} & \frac{1}{\mathcal{Q}_2(\omega - \mathcal{H} - i\epsilon)\mathcal{Q}_2} \end{pmatrix} \\ &\times \begin{pmatrix} \mathcal{P}\mathcal{H}\mathcal{Q}_1 \cdot \mathcal{Q}_1\mathcal{G}\mathcal{Q}_1 \\ \mathcal{Q}_2\mathcal{H}\mathcal{Q}_1 \cdot \mathcal{Q}_1\mathcal{G}\mathcal{Q}_1 \end{pmatrix} \end{aligned}$$

Using this result, we can find a more accurate expression for $\mathcal{H}_{\mathcal{Q}_1}$ which also contains the effects of collective vibrations into the continuum states. That is (see equation (5)),

$$\begin{aligned} \mathcal{H}_{\mathcal{Q}_1} \approx\ & \mathcal{Q}_1\mathcal{H}\mathcal{Q}_1 + \mathcal{Q}_1\mathcal{H}\mathcal{P}\frac{1}{\mathcal{P}(\omega - \mathcal{H} - i\epsilon)\mathcal{P}}\mathcal{P}\mathcal{H}\mathcal{Q}_1 \\ &+ \mathcal{Q}_1\mathcal{H}\mathcal{Q}_2\frac{1}{\mathcal{Q}_2(\omega - \mathcal{H} - i\epsilon)\mathcal{Q}_2}\mathcal{Q}_2\mathcal{H}\mathcal{Q}_1 \\ &+ \mathcal{Q}_1\mathcal{H}\mathcal{Q}_2\frac{1}{\mathcal{Q}_2(\omega - \mathcal{H} - i\epsilon)\mathcal{Q}_2}\mathcal{Q}_2\mathcal{H}\mathcal{P}\frac{1}{\mathcal{P}(\omega - \mathcal{H} - i\epsilon)\mathcal{P}}\mathcal{P}\mathcal{H}\mathcal{Q}_1 \\ &+ \mathcal{Q}_1\mathcal{H}\mathcal{P}\frac{1}{\mathcal{P}(\omega - \mathcal{H} - i\epsilon)\mathcal{P}}\mathcal{P}\mathcal{H}\mathcal{Q}_2\frac{1}{\mathcal{Q}_2(\omega - \mathcal{H} - i\epsilon)\mathcal{Q}_2}\mathcal{Q}_2\mathcal{H}\mathcal{Q}_1. \end{aligned} \tag{A.3}$$

References

[1] Nazarewicz W 2016 *J. Phys. G: Nucl. Part. Phys.* **43** 044002
[2] Roca-Maza X, Viñas X, Centelles M, Ring P and Schuck P 2011 *Phys. Rev.* C **84** 054309
[3] Roca-Maza X, Colò G and Sagawa H 2012 *Phys. Rev.* C **86** 031306

[4] Hohenberg P and Kohn W 1964 *Phys. Rev.* **136** B864–71
[5] Kohn W and Sham L J 1965 *Phys. Rev.* **140** A1133–8
[6] Engel E and Dreizler R 2011 *Density Functional Theory: An Advanced Course, Theoretical and Mathematical Physics* (Berlin: Springer)
[7] Bender M, Heenen P H and Reinhard P G 2003 *Rev. Mod. Phys.* **75** 121–80
[8] Vretenar D, Afanasjev A, Lalazissis G and Ring P 2005 *Phys. Rep.* **409** 101–259
[9] Ring P and Schuck P 2004 *The Nuclear Many-Body Problem* (Berlin: Springer)
[10] Nakatsukasa T, Inakura T and Yabana K 2007 *Phys. Rev.* C **76** 024318
[11] Colò G, Cao L, Giai N V and Capelli L 2013 *Comput. Phys. Commun.* **184** 142–61
[12] Bortignon P F, Bracco A and Broglia R A 1998 *Giant Resonances: Contemporary Concepts in Physics* (Amsterdam: Taylor & Francis)
[13] Centelles M, Roca-Maza X, Viñas X and Warda M 2009 *Phys. Rev. Lett.* **102** 122502
[14] Roca-Maza X, Centelles M, Viñas X and Warda M 2011 *Phys. Rev. Lett.* **106** 252501
[15] Roca-Maza X, Pozzi G, Brenna M, Mizuyama K and Colò G 2012 *Phys. Rev.* C **85** 024601
[16] Liang H, Zhao P, Ring P, Roca-Maza X and Meng J 2012 *Phys. Rev.* C **86** 021302
[17] Roca-Maza X *et al* 2013 *Phys. Rev.* C **87** 034301
[18] Roca-Maza X, Brenna M, Colò G, Centelles M, Viñas X, Agrawal B K, Paar N, Vretenar D and Piekarewicz J 2013 *Phys. Rev.* C **88** 024316
[19] Roca-Maza X, Viñas X, Centelles M, Agrawal B K, Colò G, Paar N, Piekarewicz J and Vretenar D 2015 *Phys. Rev.* C **92** 064304
[20] Cao L G, Roca-Maza X, Colò G and Sagawa H 2015 *Phys. Rev.* C **92** 034308
[21] Dickhoff W and Barbieri C 2004 *Prog. Part. Nucl. Phys.* **52** 377–496
[22] Lee D 2009 *Prog. Part. Nucl. Phys.* **63** 117–54
[23] Bogner S, Furnstahl R and Schwenk A 2010 *Prog. Part. Nucl. Phys.* **65** 94–147
[24] Barrett B R, Navrátil P and Vary J P 2013 *Prog. Part. Nucl. Phys.* **69** 131–81
[25] Hagen G, Papenbrock T, Hjorth-Jensen M and Dean D J 2014 *Rep. Prog. Phys.* **77** 096302
[26] Carlson J, Gandolfi S, Pederiva F, Pieper S C, Schiavilla R, Schmidt K E and Wiringa R B 2015 *Rev. Mod. Phys.* **87** 1067–118
[27] Shen S H, Hu J N, Liang H Z, Meng J, Ring P and Zhang S Q 2016 *Chin. Phys. Lett.* **33** 102103
[28] Bernard V and Giai N V 1980 *Nucl. Phys.* A **348** 75–92
[29] Colòa G, Sagawa H and Bortignon P F 2010 *Phys. Rev.* C **82** 064307
[30] Bohr A and Mottelson B 1998 *Nuclear Structure* Vol I & II (London: World Scientific)
[31] Dudek J 2016 Focus issue to celebrate the 40-year anniversary of the 1975 Nobel Prize to Aage Niels Bohr, Ben Roy Mottelson and Leo James Rainwater *Phys. Scr.* **91** 030301
[32] Bortignon P, Broglia R, Bes D and Liotta R 1977 *Phys. Rep.* **30** 305–60
[33] Bertsch G F, Bortignon P F and Broglia R A 1983 *Rev. Mod. Phys.* **55** 287–314
[34] Colò G, Van Giai N, Bortignon P F and Broglia R A 1994 *Phys. Rev.* C **50** 1496–508
[35] Moghrabi K, Grasso M, Colò G and Van Giai N 2010 *Phys. Rev. Lett.* **105** 262501
[36] Moghrabi K, Grasso M, Roca-Maza X and Colò G 2012 *Phys. Rev.* C **85** 044323
[37] Brenna M, Colò G and Roca-Maza X 2014 *Phys. Rev.* C **90** 044316
[38] Yang C J, Grasso M, Roca-Maza X, Colò G and Moghrabi K 2016 *Phys. Rev.* C **94** 034311
[39] Baldo M, Bortignon P F, Colò G, Rizzo D and Sciacchitano L 2015 *J. Phys. G: Nucl. Part. Phys.* **42** 085109
[40] Niu Y F, Colò G, Brenna M, Bortignon P F and Meng J 2012 *Phys. Rev.* C **85** 034314
[41] Mizuyama K, Colò G and Vigezzi E 2012 *Phys. Rev.* C **86** 034318
[42] Litvinova E, Ring P and Tselyaev V 2013 *Phys. Rev.* C **88** 044320
[43] Niu Y F, Colò G and Vigezzi E 2014 *Phys. Rev.* C **90** 054328
[44] Niu Y F, Colò G, Vigezzi E, Bai C L and Sagawa H 2016 *Phys. Rev.* C **94** 064328
[45] Lyutorovich N, Tselyaev V, Speth J, Krewald S, Grümmer F and Reinhard P G 2015 *Phys. Lett.* B **749** 292–7
[46] Niu Y F, Niu Z M, Colò G and Vigezzi E 2015 *Phys. Rev. Lett.* **114** 142501
[47] Brenna M, Colò G and Bortignon P F 2012 *Phys. Rev.* C **85** 014305
[48] Mahaux C, Bortignon P, Broglia R and Dasso C 1985 *Phys. Rep.* **120** 1–274
[49] Mizuyama K and Ogata K 2012 *Phys. Rev.* C **86** 041603
[50] Blanchon G, Dupuis M, Arellano H F and Vinh Mau N 2015 *Phys. Rev.* C **91** 014612
[51] Rowe D 2010 *Nuclear Collective Motion: Models and Theory* (London: Butler & Tanner)
[52] Tselyaev V I 2007 *Phys. Rev.* C **75** 024306
[53] Tselyaev V I 2013 *Phys. Rev.* C **88** 054301

[54] Litvinova E V and Tselyaev V I 2007 *Phys. Rev.* C **75** 054318
[55] Gambacurta D, Grasso M and Engel J 2015 *Phys. Rev.* C **92** 034303
[56] Lyutorovich N, Tselyaev V, Speth J, Krewald S and Reinhard P G 2016 arXiv: 1602.00862
[57] Carbone A, Colò G, Bracco A, Cao L G, Bortignon P F, Camera F and Wieland O 2010 *Phys. Rev.* C **81** 041301
[58] Bocchi G *et al* 2016 *Phys. Lett.* B **760** 273–8
[59] Blumenfeld Y, Nilsson T and Duppen P V 2013 *Phys. Scr.* **2013** 014023
[60] Litvinova E V and Afanasjev A V 2011 *Phys. Rev.* C **84** 014305
[61] Oganessian Y T and Rykaczewski K P 2015 *Phys. Today* **68** 32
[62] Harakeh M and Woude A 2001 *Giant Resonances: Fundamental High-Frequency Modes of Nuclear Excitation Oxford Science Publications* (Oxford: Oxford University Press)
[63] Yoshida S 1983 *Prog. Theor. Phys. Suppl.* **74-75** 142–56
[64] Giai N V, Bortignon P, Zardi F and Broglia R 1987 *Phys. Lett.* B **199** 155–8
[65] Bohigas O, Lane A and Martorell J 1979 *Phys. Rep.* **51** 267–316
[66] Thouless D 1961 *Nucl. Phys.* **22** 78–95
[67] Yannouleas C 1987 *Phys. Rev.* C **35** 1159–61
[68] Drozdz S, Nishizaki S, Speth J and Wambach J 1990 *Phys. Rep.* **197** 1–65
[69] Catara F, Piccitto G, Sambataro M and Van Giai N 1996 *Phys. Rev.* B **54** 17536–46
[70] Dechargé J and Gogny D 1980 *Phys. Rev.* C **21** 1568–93
[71] Nikolaus B A, Hoch T and Madland D G 1992 *Phys. Rev.* C **46** 1757–81
[72] Chabanat E, Bonche P, Haensel P, Meyer J and Schaeffer R 1998 *Nucl. Phys.* A **635** 231–56
[73] Bartel J, Quentin P, Brack M, Guet C and HÅkansson H B 1982 *Nucl. Phys.* A **386** 79–100
[74] Bertsch G and Kuo T 1968 *Nucl. Phys.* A **112** 204–8
[75] Youngblood D H, Bogucki P, Bronson J D, Garg U, Lui Y W and Rozsa C M 1981 *Phys. Rev.* C **23** 1997–2007
[76] Youngblood D H, Clark H L and Lui Y W 1999 *Phys. Rev. Lett.* **82** 691–4
[77] Khan E, Paar N, Vretenar D, Cao L G, Sagawa H and Colò G 2013 *Phys. Rev.* C **87** 064311
[78] Tamii A *et al* 2011 *Phys. Rev. Lett.* **107** 062502
[79] Rossi D M *et al* 2013 *Phys. Rev. Lett.* **111** 242503
[80] Hashimoto T *et al* 2015 *Phys. Rev.* C **92** 031305